PERGAMON

Control Engineering Practice 9 (2001) 191–198

CONTROL ENGINEERING PRACTICE

www.elsevier.com/locate/conengprac

An inverse kinematics algorithm for interaction control of a flexible arm with a compliant surface

Bruno Siciliano, Luigi Villani*

Dipartimento di Informatica e Sistemistica, Università degli Studi di Napoli Federico II, via Claudio 21, 80125 Napoli, Italy

Received 2 May 2000; accepted 1 September 2000

Abstract

This paper deals with the problem of controlling the interaction of a multilink flexible arm in contact with a compliant surface. For a given tip position and surface stiffness, the joint and deflection variables are computed using a closed-loop inverse kinematics algorithm. This is based on a suitable Jacobian matrix which includes terms accounting for the static deflections due to gravity and contact force. The computed variables are used as the set-points for a simple joint PD control, thus achieving regulation of the tip position and contact force via a joint-space controller. The scheme is tested in a simulation case study for a planar two-link manipulator. © *2001 Elsevier Science Ltd. All rights reserved.*

Keywords: Flexible arms; Position control; Force control; Inverse kinematics.

1. Introduction

Lightweight flexible arms are preferred to bulky rigid arms when high-speed, low-energy consumption, large workspace and high payload-to-arm weight are required. They have captured the attention of several researchers in the last decade, since they pose a number of challenging issues from a modelling and control standpoint (Book, 1993; Canudas de Wit, Siciliano & Bastin, 1996).

A notable feature of flexible arms is that the system configuration cannot be completely described by the joint variables and additional deflection variables must be introduced to take into account for links deformation. Moreover, to obtain a finite-dimensional model, suitable approximations of the modes of link deformation have to be made. On the other hand, since the number of control inputs is strictly less than the number of mechanical degrees-of-freedom, the control design is much more complex than for rigid arms.

Typically the actuators are co-located at the joints and thus the most effective control strategies for flexible arms have been developed at the joint level, both for the problems of regulation (De Luca & Siciliano, 1993a; De Luca & Panzieri, 1996) and tracking (Siciliano & Book, 1988; De Luca & Siciliano, 1993b; Khorrami & Jain, 1993; Vandegrift, Lewis & Zhu, 1994). Therefore, when a desired position is specified for the tip, the corresponding joint and deflection variables to be used as inputs for the joint-space controller have to be found by solving an inverse kinematics problem. This can be conveniently formulated in differential form by deriving a suitable Jacobian that relates the joint and deflection rates to the tip rate.

In a previous work by Siciliano (1994), the case of a flexible arm moving in free space under gravity has been considered. A solution based on the well-known closed-loop inverse kinematics (CLIK) scheme developed for rigid arms was proposed. The main feature is the adoption of a Jacobian obtained by correcting the equivalent rigid arm Jacobian with a term accounting for the static deflections due to gravity. When the arm interacts with the environment, the additional deflections caused by the contact forces must be suitably taken into account for the computation of the inverse kinematic solution. This can be done by adding another correcting term to the Jacobian both in the case of infinitely stiff environment (Siciliano, 1999) and compliant environment (Siciliano, 1998).

In this work the case of a robot arm in contact with a compliant environment is considered. Assuming a simple elastic model for the contact surface, a position

* Corresponding author. Tel.: +39-081-7683635; fax: +39-081-7683186.

E-mail addresses: siciliano@unina.it (B. Siciliano), lvillani@unina.it (L. Villani).

0967-0661/01/$ - see front matter © 2001 Elsevier Science Ltd. All rights reserved.
PII: S0967-0661(00)00097-6

set-point is assigned, corresponding to the desired force applied to the desired point on the surface. Then a closed-loop inverse kinematics algorithm based on the well-known transpose Jacobian scheme described in Siciliano (1990) is adopted to compute the joint and deflection variables. These are input to a simple proportional-derivative (PD) joint regulator (De Luca & Siciliano, 1993a). In sum, force and position regulation are achieved in an indirect way as long as the arm kinematic model, the mass distribution and stiffness of the links as well as the environment stiffness and position are known.

Notice that one of the attractive features of the proposed approach is that, similar to the rigid arm case, any Jacobian-based inverse kinematics scheme can be adopted in principle, as well as any joint-space control law. The solution chosen in this work for kinematic inversion does not require the inverse of the Jacobian and thus it works well on the neighborhood of singularities. Moreover, the PD regulator does not use deflection measurements; however, it ensures asymptotic stability only in the presence of significant damping. When passive damping is too low, active vibration damping can be achieved by using full state-feedback (Canudas et al., 1996).

A planar two-link flexible arm in contact with a compliant surface is considered to develop a case study with different values of surface stiffness.

2. Modelling

For the purpose of this work, planar n-link flexible manipulators with revolute joints are considered. The links are only subject to bending deformations in the plane of motion, i.e. torsional effects are neglected. A sketch of a two-link arm, with coordinate frame assignment, is shown in Fig. 1. The rigid motion is described by the joint angles ϑ_i, while $w_i(x_i)$ denotes the transversal deflection of link i at x_i, $0 \leqslant x_i \leqslant \ell_i$, ℓ_i being the link length.

Let $\mathbf{p}_i^i(x_i) = [x_i \; w_i(x_i)]^{\mathrm{T}}$ be the position of a point along the deflected link i with respect to frame (X_i, Y_i) and $\mathbf{p}_i$ be the position of the same point in the base frame. Also let $\mathbf{r}_{i+1}^i = \mathbf{p}_i^i(\ell_i)$ be the position of the origin of frame (X_{i+1}, Y_{i+1}) with respect to frame (X_i, Y_i), and $\mathbf{r}_{i+1}$ its position in the base frame.

The joint (rigid) rotation matrix $\mathbf{R}_i$ and the rotation matrix $\mathbf{E}_i$ of the (flexible) link at the end point are, respectively,

$$\mathbf{R}_i = \begin{bmatrix} \cos\vartheta_i & -\sin\vartheta_i \\ \sin\vartheta_i & \cos\vartheta_i \end{bmatrix} \tag{1}$$

and

$$\mathbf{E}_i = \begin{bmatrix} 1 & -w'_{ie} \\ w'_{ie} & 1 \end{bmatrix}, \tag{2}$$

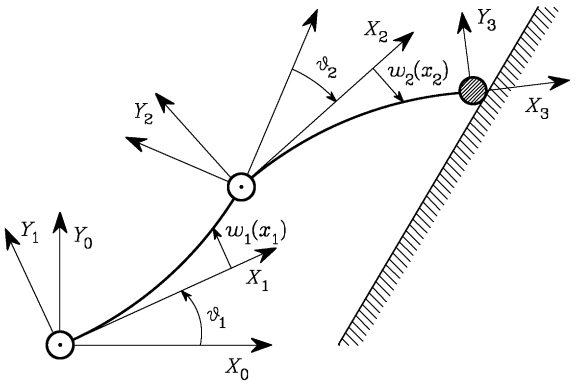

Fig. 1. Planar two-link flexible arm.

where $w'_{ie} = (\partial w_i/\partial x_i)|_{x_i=\ell_i}$, and the small deflection approximation $\arctan w'_{ie} \simeq w'_{ie}$ has been made. Hence the above absolute position vectors can be expressed as

$$\mathbf{p}_i = \mathbf{r}_i + \mathbf{W}_i \mathbf{p}_i^i \tag{3}$$

and

$$\mathbf{r}_{i+1} = \mathbf{r}_i + \mathbf{W}_i \mathbf{r}_{i+1}^i, \tag{4}$$

where $\mathbf{W}_i$ is the global transformation matrix from the base frame to (X_i, Y_i) given by the recursive equation

$$\mathbf{W}_i = \mathbf{W}_{i-1}\mathbf{E}_{i-1}\mathbf{R}_i = \hat{\mathbf{W}}_{i-1}\mathbf{R}_i \tag{5}$$

with

$$\hat{\mathbf{W}}_0 = \mathbf{I}. \tag{6}$$

On the basis of the above relations, the kinematics of any point along the manipulator is completely specified as a function of joint angles and link deflections.

A finite-dimensional model (of order m_i) of link flexibility can be obtained by the assumed modes technique. By exploiting the separability in time and space of solutions to the Euler–Bernoulli equation for flexible beams

$$(EI)_i \frac{\partial^4 w_i(x_i,t)}{\partial x_i^4} + \rho_i \frac{\partial^2 w_i(x_i,t)}{\partial t^2} = 0 \tag{7}$$

for $i = 1, \ldots, n$ where ρ_i is the uniform density and $(EI)_i$ is the constant flexural rigidity of link i, the link deflection can be expressed as

$$w_i(x_i,t) = \sum_{j=1}^{m_i} \phi_{ij}(x_i)\delta_{ij}(t), \tag{8}$$

where $\delta_{ij}(t)$ are the time-varying variables associated with the assumed spatial mode shapes $\phi_{ij}(x_i)$ of link i. The mode shapes have to satisfy proper boundary conditions at the base (clamped) and at the end of each link (mass).

In view of (8), a direct kinematics equation can be derived expressing the position $\mathbf{p}$ of the manipulator tip

point as a function of the $(n\times 1)$ joint variable vector $\boldsymbol{\vartheta}$ and the $(m\times 1)$ deflection variable vector $\boldsymbol{\delta}$, i.e.

$$\mathbf{p}=\mathbf{k}(\boldsymbol{\vartheta},\boldsymbol{\delta}), \tag{9}$$

where $m=\sum_{i=1}^{n} m_i$.

For later use in the inverse kinematics scheme, also the differential kinematics is needed. The absolute linear velocity of an arm point is

$$\dot{\mathbf{p}}_i=\dot{\mathbf{r}}_i+\dot{\mathbf{W}}_i\mathbf{p}_i^i+\mathbf{W}_i\dot{\mathbf{p}}_i^i \tag{10}$$

with $\dot{\mathbf{r}}_{i+1}^i=\dot{\mathbf{p}}_i^i(\ell_i)$. Since the links are assumed inextensible ($\dot{x}_i=0$), then $\dot{\mathbf{p}}_i^i(x_i)=[0\ \dot{w}_i(x_i)]^{\mathrm{T}}$. The computation of (10) takes advantage of the recursion

$$\dot{\mathbf{W}}_i=\hat{\dot{\mathbf{W}}}_{i-1}\mathbf{R}_i+\hat{\mathbf{W}}_{i-1}\dot{\mathbf{R}}_i \tag{11}$$

with

$$\hat{\dot{\mathbf{W}}}_i=\dot{\mathbf{W}}_i\mathbf{E}_i+\mathbf{W}_i\dot{\mathbf{E}}_i. \tag{12}$$

Also, note that

$$\dot{\mathbf{R}}_i=\mathbf{S}\mathbf{R}_i\dot{\vartheta}_i,\quad \dot{\mathbf{E}}_i=\mathbf{S}\dot{w}'_{ie} \tag{13}$$

with

$$\mathbf{S}=\begin{bmatrix}0 & -1\\ 1 & 0\end{bmatrix}. \tag{14}$$

In view of (9)–(14), it is not difficult to show that the differential kinematics equation expressing the tip velocity $\dot{\mathbf{p}}$ as a function of $\dot{\boldsymbol{\vartheta}}$ and $\dot{\boldsymbol{\delta}}$, can be written in the form

$$\dot{\mathbf{p}}=\mathbf{J}_{\vartheta}(\boldsymbol{\vartheta},\boldsymbol{\delta})\dot{\boldsymbol{\vartheta}}+\mathbf{J}_{\delta}(\boldsymbol{\vartheta},\boldsymbol{\delta})\dot{\boldsymbol{\delta}}, \tag{15}$$

where $\mathbf{J}_{\vartheta}=\partial\mathbf{k}/\partial\boldsymbol{\vartheta}$ and $\mathbf{J}_{\delta}=\partial\mathbf{k}/\partial\boldsymbol{\delta}$.

Assume that the manipulator is in contact with the environment. By virtue of the virtual work principle, the vector $\mathbf{f}$ of the forces exerted by the manipulator on the environment performing work on $\mathbf{p}$ has to be related to the $(n\times 1)$ vector $\mathbf{J}_{\vartheta}^{\mathrm{T}}\mathbf{f}$ of joint torques performing work on $\boldsymbol{\vartheta}$ and the $(m\times 1)$ vector $\mathbf{J}_{\delta}^{\mathrm{T}}\mathbf{f}$ of the elastic reaction forces performing work on $\boldsymbol{\delta}$.

A finite-dimensional Lagrangian dynamic model of the planar manipulator in contact with the environment can be obtained in terms of $\boldsymbol{\vartheta}$ and $\boldsymbol{\delta}$ in the form (De Luca & Siciliano, 1991)

$$\begin{aligned}&\mathbf{B}_{\vartheta\vartheta}(\boldsymbol{\vartheta},\boldsymbol{\delta})\ddot{\boldsymbol{\vartheta}}+\mathbf{B}_{\vartheta\delta}(\boldsymbol{\vartheta},\boldsymbol{\delta})\ddot{\boldsymbol{\delta}}+\mathbf{c}_{\vartheta}(\boldsymbol{\vartheta},\boldsymbol{\delta},\dot{\boldsymbol{\vartheta}},\dot{\boldsymbol{\delta}})\\ &\quad+\mathbf{g}_{\vartheta}(\boldsymbol{\vartheta},\boldsymbol{\delta})=\boldsymbol{\tau}-\mathbf{J}_{\vartheta}^{\mathrm{T}}(\boldsymbol{\vartheta},\boldsymbol{\delta})\mathbf{f},\end{aligned} \tag{16}$$

$$\begin{aligned}&\mathbf{B}_{\vartheta\delta}^{\mathrm{T}}(\boldsymbol{\vartheta},\boldsymbol{\delta})\ddot{\boldsymbol{\vartheta}}+\mathbf{B}_{\delta\delta}(\boldsymbol{\vartheta},\boldsymbol{\delta})\ddot{\boldsymbol{\delta}}+\mathbf{c}_{\delta}(\boldsymbol{\vartheta},\boldsymbol{\delta},\dot{\boldsymbol{\vartheta}},\dot{\boldsymbol{\delta}})\\ &\quad+\mathbf{g}_{\delta}(\boldsymbol{\vartheta},\boldsymbol{\delta})+\mathbf{D}\dot{\boldsymbol{\delta}}+\mathbf{K}\boldsymbol{\delta}=-\mathbf{J}_{\delta}^{\mathrm{T}}(\boldsymbol{\vartheta},\boldsymbol{\delta})\mathbf{f}.\end{aligned} \tag{17}$$

where $\mathbf{B}_{\vartheta\vartheta}$, $\mathbf{B}_{\vartheta\delta}$, $\mathbf{B}_{\delta\delta}$ are the matrix blocks of the positive-definite symmetric inertia matrix, $\mathbf{c}_{\vartheta}$, $\mathbf{c}_{\delta}$ are the vectors of Coriolis and centrifugal forces, $\mathbf{g}_{\vartheta}$, $\mathbf{g}_{\delta}$ are the vector of gravitational forces, $\mathbf{K}$ is the diagonal and positive definite link stiffness matrix, $\mathbf{D}$ is the diagonal and positive-semidefinite link damping matrix, and $\boldsymbol{\tau}$ is the vector of the input joint torques.

3. Interaction with the environment

Consider the situation when the arm tip is in contact with a frictionless and compliant planar surface. By assuming a point contact, a simple model of the elastic force is

$$\mathbf{f}=k_e\mathbf{n}\mathbf{n}^{\mathrm{T}}(\mathbf{p}-\mathbf{p}_e)=k_e\mathbf{n}\mathbf{n}^{\mathrm{T}}(\mathbf{k}(\boldsymbol{\vartheta},\boldsymbol{\delta})-\mathbf{p}_e), \tag{18}$$

where k_e is the surface stiffness, $\mathbf{p}_e$ is the undeformed (constant) position of the surface, $\mathbf{n}$ is the (constant) unit vector of the direction normal to the surface, and the direct kinematics Eq. (9) has been used to express the position of the contact point in terms of joint and deflection variables. Also, it is assumed that contact is not lost.

By virtue of (17), in a static situation the deflections satisfy the equation

$$\mathbf{g}_{\delta}(\boldsymbol{\vartheta},\boldsymbol{\delta})+\mathbf{K}\boldsymbol{\delta}=-\mathbf{J}_{\delta}^{\mathrm{T}}(\boldsymbol{\vartheta},\boldsymbol{\delta})\mathbf{f}. \tag{19}$$

According to the small deflection approximation, it can be assumed that $\mathbf{g}_{\delta}$ is only a function of $\boldsymbol{\vartheta}$ (De Luca & Siciliano, 1993a) and so is the case for $\mathbf{J}_{\delta}$ in (15) and $\mathbf{p}$ in (18). Hence, the deflection variables can be computed from (19) as

$$\boldsymbol{\delta}=-\mathbf{K}^{-1}(k_e\boldsymbol{J}_{\delta n}(\boldsymbol{\vartheta})(p_n(\boldsymbol{\vartheta})-p_{en})+\mathbf{g}_{\delta}(\boldsymbol{\vartheta})) \tag{20}$$

where

$$\boldsymbol{J}_{\delta n}=\mathbf{J}_{\delta}^{\mathrm{T}}\mathbf{n},\quad p_n=\mathbf{n}^{\mathrm{T}}\mathbf{p},\quad p_{en}=\mathbf{n}^{\mathrm{T}}\mathbf{p}_e. \tag{21}$$

For later use in the inverse kinematics scheme, differentiating (20) with respect to time gives

$$\dot{\boldsymbol{\delta}}=\mathbf{J}_{fg}(\boldsymbol{\vartheta})\dot{\boldsymbol{\vartheta}}, \tag{22}$$

where

$$\mathbf{J}_{fg}=-\mathbf{K}^{-1}(k_e\mathbf{J}_f(\boldsymbol{\vartheta})+\mathbf{J}_g(\boldsymbol{\vartheta})) \tag{23}$$

with

$$\mathbf{J}_f=\frac{\partial\boldsymbol{J}_{\delta n}}{\partial\boldsymbol{\vartheta}}(p_n-p_{en})+\boldsymbol{J}_{\delta n}\frac{\partial p_n}{\partial\boldsymbol{\vartheta}} \tag{24}$$

and $\mathbf{J}_g=\partial\mathbf{g}_{\delta}/\partial\boldsymbol{\vartheta}$. Folding (22) into (15) yields

$$\dot{\mathbf{p}}=\mathbf{J}_p(\boldsymbol{\vartheta},\boldsymbol{\delta})\dot{\boldsymbol{\vartheta}} \tag{25}$$

where

$$\mathbf{J}_p=\mathbf{J}_{\vartheta}+\mathbf{J}_{\delta}\mathbf{J}_{fg} \tag{26}$$

is the overall Jacobian matrix relating joint velocity to tip velocity. Notice that the Jacobian in (26) is obtained by modifying the rigid-body Jacobian $\mathbf{J}_{\vartheta}$ with two terms that account for the deflections induced by the contact force and gravity, respectively. The differential kinematics (25) is the basic model that is used below to derive an inverse kinematics solution scheme.

4. Interaction control

The control objective can be specified in terms of a desired force $f_d\mathbf{n}$ aligned with $\mathbf{n}$ and a desired position $\mathbf{p}_d$ on the contact plane. Nevertheless, the quantities f_d and $\mathbf{p}_d$ cannot be assigned independently, since they have to be consistent with the model of the elastic force (18). In other words, the desired value of force f_d can be achieved only if the component normal to the plane of the desired position $\mathbf{p}_d$ is chosen as

$$p_{dn} = \mathbf{n}^{\mathrm{T}}\mathbf{p}_d = k_e^{-1} f_d + p_{en}, \tag{27}$$

thus force control is realized indirectly via position control.

The control scheme proposed in this paper is composed of two stages. The first stage is in charge of solving the inverse kinematics problem to compute the desired vectors of joint variables $\boldsymbol{\vartheta}_d$ and deflection variables $\boldsymbol{\delta}_d$ that place the flexible arm tip at the desired position $\mathbf{p}_d$. These variables are used as the set-points for the second stage, which is a simple *PD* joint regulator.

The attractive feature of the differential kinematics Eq. (25) is its formal analogy with the differential kinematics equation for a rigid arm. Therefore, any Jacobian-based inverse kinematics scheme can be adopted in principle. In this respect, one of the most effective schemes is the closed-loop inverse kinematics (CLIK) scheme (Siciliano, 1990) that reformulates the inverse kinematics problem in terms of the convergence of a suitable closed-loop dynamic system.

According to the Jacobian transpose scheme, the joint variables vector is computed by integrating the joint velocity vector chosen as

$$\dot{\boldsymbol{\vartheta}} = \mathbf{J}_p^{\mathrm{T}}(\boldsymbol{\vartheta}, \boldsymbol{\delta})\mathbf{K}_p(\mathbf{p}_d - \mathbf{p}). \tag{28}$$

By using a Lyapunov argument (Sicilano, 1990) it can be shown that, as long as the vector $\mathbf{K}_p(\mathbf{p}_d - \mathbf{p})$ is outside the null space of $\mathbf{J}_p^{\mathrm{T}}$, the tip position error $\mathbf{p} - \mathbf{p}_d$ asymptotically tends to zero. In fact, a suitable choice of the matrix $\mathbf{K}_p$ can be made to avoid that the scheme gets stuck with $\mathbf{p}_d - \mathbf{p} \neq 0$ and $\dot{\boldsymbol{\vartheta}} = 0$.

In sum, $\boldsymbol{\vartheta}$ and $\boldsymbol{\delta}$ tend asymptotically to the constant values $\boldsymbol{\delta}_d$ and $\mathbf{p}_d$ such that $\mathbf{p}_d = \mathbf{k}(\boldsymbol{\theta}_d, \boldsymbol{\delta}_d)$.

It is worth remarking that if the desired tip position is time-varying, a similar Lyapunov argument can be worked out to show that the tracking error can be made arbitrarily small by augmenting the feedback gains in the matrix $\mathbf{K}_p$, whereas at steady state asymptotic convergence is still obtained. In practical implementation, bounds exist on the largest values of the gains in $\mathbf{K}_p$ depending on the sampling time at which the scheme is discretized.

The computed values of $\boldsymbol{\theta}_d$ and $\boldsymbol{\omega}_d$ are input to the simple PD regulator (De Luca & Siciliano, 1993a)

$$\boldsymbol{\tau} = \mathbf{K}_1(\boldsymbol{\vartheta}_d - \boldsymbol{\vartheta}) - \mathbf{K}_2\dot{\boldsymbol{\vartheta}} + \mathbf{g}_{\vartheta}(\boldsymbol{\vartheta}_d, \boldsymbol{\delta}_d) + \mathbf{J}_{\vartheta}^{\mathrm{T}}(\boldsymbol{\vartheta}_d, \boldsymbol{\delta}_d) f_d\mathbf{n}, \tag{29}$$

where $\mathbf{K}_1$ and $\mathbf{K}_2$ are suitable positive-definite matrix gains. The feedforward terms $\mathbf{g}_{\vartheta}(\boldsymbol{\vartheta}_d, \boldsymbol{\delta}_d)$ and $\mathbf{J}_{\vartheta}^{\mathrm{T}}(\boldsymbol{\vartheta}_d, \boldsymbol{\delta}_d) f_d\mathbf{n}$ are required to compensate for the gravity torque and contact force, respectively, at steady state.

The control law (29) ensures asymptotic convergence of $\boldsymbol{\theta}$ and $\boldsymbol{\delta}$ to the corresponding set-points. Hence, the two-stages control scheme (28), (29) guarantees that $\mathbf{p} \to \mathbf{p}_d$ and $\mathbf{f} \to \mathbf{f}_d$ as $t \to \infty$.

It is worth remarking that the proposed scheme only makes use of joint position and velocity measurements. Obviously, any joint position control law for flexible arms may be used in the second stage of the scheme in lieu of the simple PD regulator adopted in this work. In any case, the overall performance in terms of tip position and force errors strongly depends on the accuracy of the static model of the flexible arm, as well as on the accuracy of the available estimates of the stiffness and position of the contact surface.

5. Case study

In order to test the proposed inverse kinematics scheme, a planar two-link flexible arm (Fig. 1) is considered:

$$\boldsymbol{\vartheta} = [\vartheta_1 \quad \vartheta_2]^{\mathrm{T}}.$$

In the following, all the data of the arm required for the implementation of the proposed control scheme are given. The complete dynamic model used in the simulation can be found in De Luca and Siciliano (1991).

The following parameters are set up for the links and a payload which is assumed to be placed at the tip of the flexible arm:

$\rho_1 = \rho_2 = 1.0$ kg/m (link uniform density),
$\ell_1 = \ell_2 = 0.5$ m (link length),
$d_1 = d_2 = 0.25$ m (link center of mass),
$m_1 = m_2 = 0.5$ m (link mass),
$m_{h1} = m_{h2} = 1$ kg (hub mass),
$m_p = 0.1$ kg (payload mass),
$(EI)_1 = (EI)_2 = 10$ Nm^2 (flexural link rigidity).

An expansion with two clamped-mass assumed modes is taken for each link:

$$\boldsymbol{\delta} = [\delta_{11} \quad \delta_{12} \quad \delta_{21} \quad \delta_{22}]^{\mathrm{T}}.$$

The resulting natural frequencies of vibration are

$$f_{11} = 1.40 \text{ Hz}, \quad f_{12} = 5.10 \text{ Hz},$$

$$f_{21} = 5.21 \text{ Hz}, \quad f_{22} = 32.46 \text{ Hz}.$$

The stiffness coefficients of the diagonal matrix $\mathbf{K}$ in (17) are

$$k_{11} = 38.79 \text{ N}, \quad k_{12} = 513.37 \text{ N},$$

$$k_{21} = 536.09 \text{ N}, \quad k_{22} = 20792.09 \text{ N}.$$

The link end-point deflections and their spatial derivatives can be expressed as

$$w_{1e} = \phi_{11,e}\delta_{11} + \phi_{12,e}\delta_{12},$$
$$w_{2e} = \phi_{21,e}\delta_{21} + \phi_{22,e}\delta_{22},$$
$$w'_{1e} = \phi'_{11,e}\delta_{11} + \phi'_{12,e}\delta_{12},$$
$$w'_{2e} = \phi'_{21,e}\delta_{21} + \phi'_{22,e}\delta_{22},$$

where the constants are

$$\phi_{11,e} = 0.39, \quad \phi_{12,e} = 0.36,$$
$$\phi'_{11,e} = 1.34, \quad \phi'_{12,e} = -1.38,$$
$$\phi_{21,e} = 1.49, \quad \phi_{22,e} = -0.75,$$
$$\phi'_{21,e} = 4.30, \quad \phi'_{22,e} = -15.49.$$

The tip position in (9) is expressed by

$$\mathbf{p} = \mathbf{R}_1(\vartheta_1)(\mathbf{r}_2^1(\delta_{11},\delta_{12}) + \mathbf{E}_1(\delta_{11},\delta_{12})\mathbf{R}_2(\vartheta_2)\mathbf{r}_3^2(\delta_{21},\delta_{22})), \tag{30}$$

where the position vectors and the rotation matrices can be computed as illustrated in Section 2. The Jacobians in (15) resulting from (30) are

$$\mathbf{J}_\vartheta = \begin{bmatrix} \dfrac{\mathrm{d}\mathbf{R}_1}{\mathrm{d}\vartheta_1}(\mathbf{r}_2^1 + \mathbf{E}_1\mathbf{R}_2\mathbf{r}_3^2) \\ \mathbf{R}_1(\mathbf{E}_1\dfrac{\mathrm{d}\mathbf{R}_2}{\mathrm{d}\vartheta_2}\mathbf{r}_3^2) \end{bmatrix}^{\mathrm{T}} \tag{31}$$

and

$$\mathbf{J}_\delta = \begin{bmatrix} \mathbf{R}_1\left(\dfrac{\partial\mathbf{r}_2^1}{\partial\delta_{11}} + \dfrac{\partial\mathbf{E}_1}{\partial\delta_{11}}\mathbf{R}_2\mathbf{r}_3^2\right) \\ \mathbf{R}_1\left(\dfrac{\partial\mathbf{r}_2^1}{\partial\delta_{12}} + \dfrac{\partial\mathbf{E}_1}{\partial\delta_{12}}\mathbf{R}_2\mathbf{r}_3^2\right) \\ \mathbf{R}_1\mathbf{E}_1\mathbf{R}_2\dfrac{\partial\mathbf{r}_3^2}{\partial\delta_{21}} \\ \mathbf{R}_1\mathbf{E}_1\mathbf{R}_2\dfrac{\partial\mathbf{r}_3^2}{\partial\delta_{22}} \end{bmatrix}^{\mathrm{T}}, \tag{32}$$

where the required derivatives are easy to compute.

The following coefficients are also needed for the gravity term:

$$v_{ij} = \int_0^{\ell_i} \rho_i\phi_{ij}(x_i)\,\mathrm{d}x_i, \quad i,j = 1,2.$$

With the above data, they take on the values:

$$v_{11} = 0.069, \quad v_{12} = 0.12,$$
$$v_{21} = 0.28, \quad v_{22} = 0.30.$$

The resulting gravity term is (standard abbreviations are used for sine and cosine)

$$\mathbf{g}_\vartheta = [g_1 \quad g_2]^{\mathrm{T}},$$
$$\mathbf{g}_\delta = [g_3 \quad g_4 \quad g_5 \quad g_6]^{\mathrm{T}}$$

with

$$g_1 = g_{11}c_1 + (g_{12}\delta_{11} + g_{13}\delta_{12})s_1 + g_{14}c_{12} + (g_{15}\delta_{11} + g_{16}\delta_{12} + g_{17}\delta_{21} + g_{18}\delta_{22})s_{12},$$
$$g_2 = g_{21}c_{12} + (g_{22}\delta_{11} + g_{23}\delta_{12} + g_{24}\delta_{21} + g_{25}\delta_{22})s_{12},$$
$$g_3 = g_{31}c_1 + g_{32}c_{12},$$
$$g_4 = g_{41}c_1 + g_{42}c_{12},$$
$$g_5 = g_{51}c_{12},$$
$$g_6 = g_{61}c_{12},$$

where the constant coefficients are

$$g_{11} = g_0(m_1d_1 + (m_2 + m_{h2} + m_p)\ell_1),$$
$$g_{12} = -g_0((m_2 + m_{h2} + m_p)\phi_{11e} + v_{11}),$$
$$g_{13} = -g_0((m_2 + m_{h2} + m_p)\phi_{12e} + v_{12}),$$
$$g_{14} = g_0(m_2d_2 + m_p\ell_2),$$
$$g_{15} = -g_0(m_2d_2 + m_p\ell_2)\phi'_{11,e},$$
$$g_{16} = -g_0(m_2d_2 + m_p\ell_2)\phi'_{12,e},$$
$$g_{17} = -g_0(m_p\phi_{21,e} + v_{21}),$$
$$g_{18} = -g_0(m_p\phi_{22,e} + v_{22}),$$
$$g_{21} = g_0(m_2d_2 + m_p\ell_2),$$
$$g_{22} = -g_0(m_2d_2 + m_p\ell_2)\phi'_{11,e},$$
$$g_{23} = -g_0(m_2d_2 + m_p\ell_2)\phi'_{12,e},$$
$$g_{24} = -g_0(m_p\phi_{21,e} + v_{21}),$$
$$g_{25} = -g_0(m_p\phi_{22,e} + v_{22}),$$
$$g_{31} = g_0((m_2 + m_{h2} + m_p)\phi_{11,e} + v_{11}),$$
$$g_{32} = g_0(m_2d_2 + m_p\ell_2)\phi'_{11,e},$$
$$g_{41} = g_0((m_2 + m_{h2} + m_p)\phi_{12,e} + v_{12}),$$
$$g_{42} = g_0(m_2d_2 + m_p\ell_2)\phi'_{12,e},$$
$$g_{51} = g_0(m_p\phi_{21,e} + v_{21}),$$
$$g_{61} = g_0(m_p\phi_{22,e} + v_{22}),$$

g_0 being the gravity acceleration. It is worth noticing that $\mathbf{g}_\delta$ is only a function of $\boldsymbol{\vartheta}$, as anticipated.

The Jacobian resulting from $\mathbf{g}_\delta$ is

$$\mathbf{J}_g = \begin{bmatrix} -g_{11}s_1 - g_{12}s_{12} & -g_{12}s_{12} \\ -g_{21}s_1 - g_{22}s_{12} & -g_{22}s_{12} \\ -g_{31}s_{12} & -g_{31}s_{12} \\ -g_{41}s_{12} & -g_{41}s_{12} \end{bmatrix}. \tag{33}$$

The contact surface is a vertical plane, thus the normal vector in (18) is $\mathbf{n} = [1 \quad 0]^{\mathrm{T}}$; a point of the undeformed plane is

$$\mathbf{p}_o = [0.55 \quad 0]^{\mathrm{T}} \text{ m}$$

and the contact stiffness is $k_e = 50$ N/m.

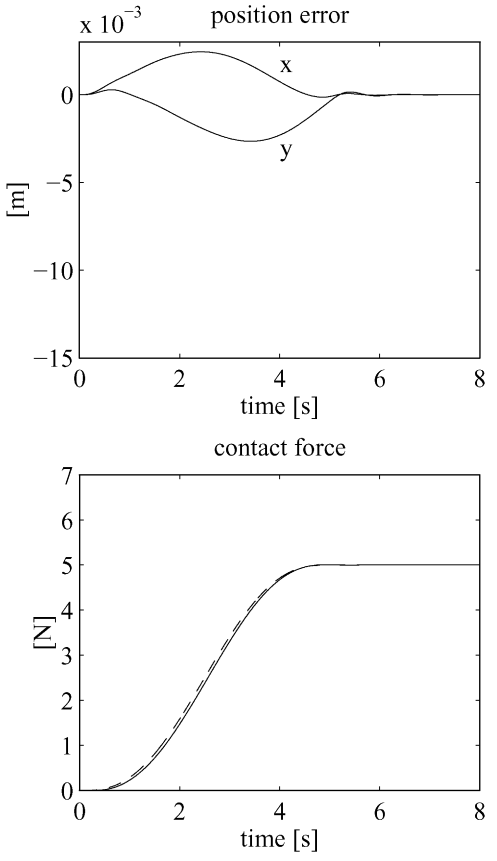

Fig. 2. Time histories of the position error, actual (solid line) and desired (dashed line) contact force for the first example.

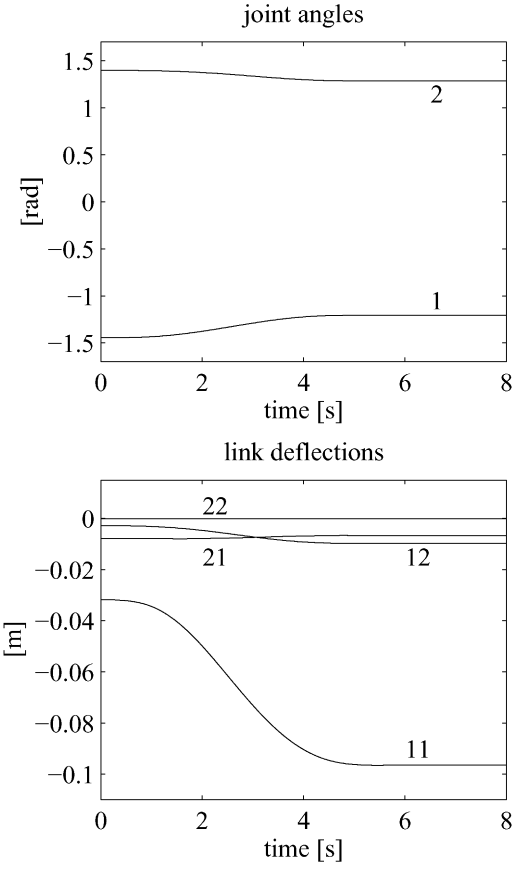

Fig. 3. Time histories of the joint angles and link deflections for the first example.

With the expressions in (31)–(33) and (24), the overall Jacobian in (26) can be easily computed.

The feedback matrix gain in (28) is chosen as

$$\mathbf{K}_p = \mathrm{diag}\{500, 500\}$$

and the inverse kinematics scheme is discretized at a sampling time $T_c = 1$ ms, using Euler integration rule. In particular, according to (28), the joint variables vector $\boldsymbol{\vartheta}_d$ is computed as

$$\boldsymbol{\vartheta}_d(t_{k+1}) = \boldsymbol{\vartheta}_d(t_k) + T_c \mathbf{J}_p^{\mathrm{T}}(\boldsymbol{\vartheta}_d(t_k), \boldsymbol{\delta}_d(t_k))\mathbf{K}_p(\mathbf{p}_d(t_k) - \mathbf{p}(t_k))$$

and, according to (20), the deflection variables vector $\boldsymbol{\delta}_d$ is computed as

$$\boldsymbol{\delta}_d(t_{k+1}) = -\mathbf{K}^{-1}(k_{eJ\delta n}(\boldsymbol{\vartheta}_d(t_k))(p_n(t_k) - p_{en}) + \mathbf{g}_\delta(\boldsymbol{\vartheta}_d(t_k))).$$

The feedback matrix gains in (29) are chosen as

$$\mathbf{K}_1 = \mathrm{diag}\{25, 25\}, \quad \mathbf{K}_2 = \mathrm{diag}\{3, 3\}.$$

Numerical simulations have been performed using MATLAB with Simulink.

In the first example, it is assumed that the stiffness of the environment is known.

The arm is initially placed with the tip in contact with the undeformed plane in the position

$$\mathbf{p}(0) = [0.55 \quad -0.55]^{\mathrm{T}} \text{ m}$$

with null contact force; the corresponding generalized coordinates of the arm (computed by using the CLIK algorithm (28)) are

$$\boldsymbol{\vartheta} = [-1.4448 \quad 1.3967]^{\mathrm{T}} \text{ rad},$$

$$\boldsymbol{\delta} = [-0.0319 \quad -0.0029 \quad -0.0078 \quad -0.0001]^{\mathrm{T}} \text{ m}.$$

The desired tip position is

$$\mathbf{p}_d = [0.65 \quad -0.50]^{\mathrm{T}} \text{ m},$$

hence, the corresponding desired force is

$$\mathbf{f}_d = [5 \quad 0]^{\mathrm{T}} \text{ N}$$

and a fifth-order polynomial trajectory with null initial and final velocity and acceleration is imposed from the initial to the final position with a duration of 5 s.

The resulting time histories of the position errors and of the actual and desired contact force are reported in Fig. 2, and the time histories of the joint angles and link deflections are reported in Fig. 3.

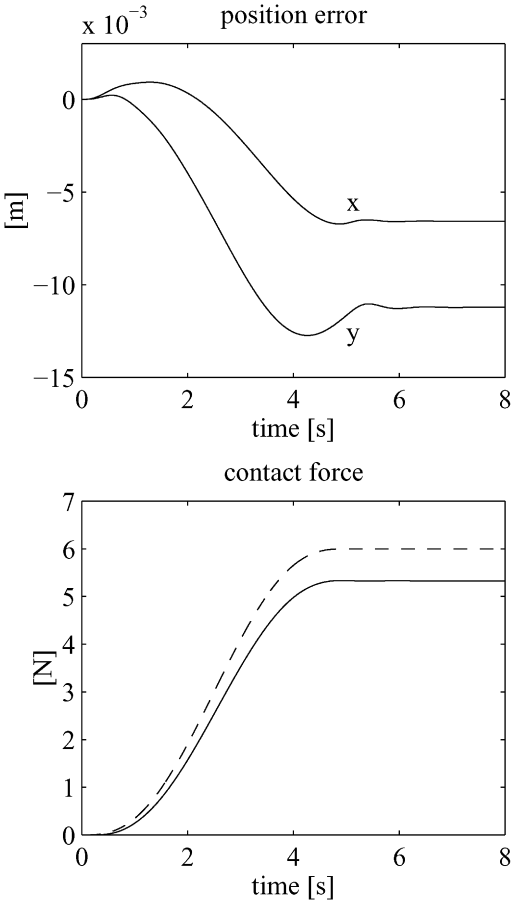

Fig. 4. Time histories of the position error, actual (solid line) and desired (dashed line) contact force for the second example.

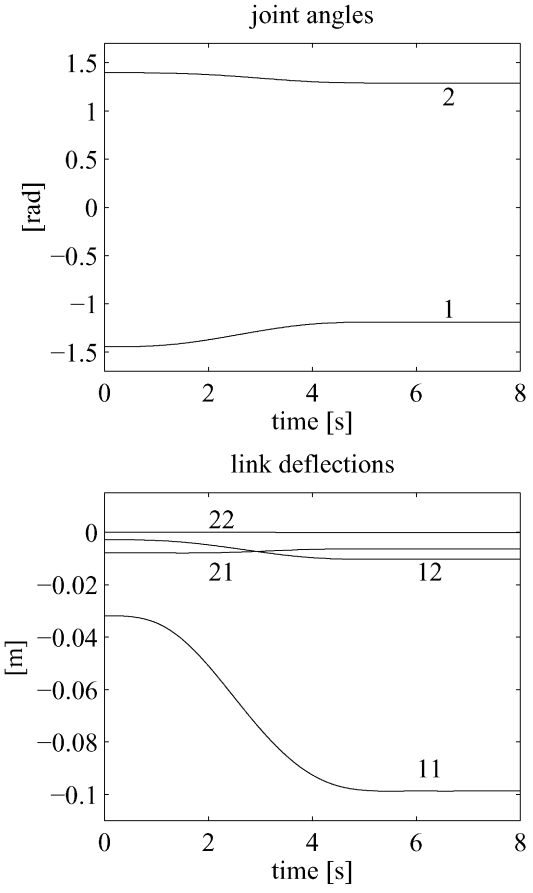

Fig. 5. Time histories of the joint angles and link deflections for the second example.

It can be recognized that the tracking error along the trajectory is small, and both the desired force and position are reached at steady state. Notice also that, because of gravity and contact force, the arm has to bend to reach the desired tip position properly. Actually the bending is much larger on the first link as expected (the links have the same parameters).

In the second numerical example, all the data are the same except for the estimated contact stiffness which is assumed to be 60 N/m in lieu of the true value of 50 N/m. Hence, the desired force

$$\mathbf{f}_d = [6 \quad 0]^{\mathrm{T}} \text{ N}$$

is expected, with the same desired position.

The resulting time histories of the position errors and of the actual (solid line) and desired (dashed line) contact force are reported in Fig. 4, and the time histories of the joint angles and link deflections are reported in Fig. 5.

It can be seen that the tracking error along the trajectory is limited, but a constant offset remains at steady state. Accordingly, the contact force reaches a constant value that is lower than the desired one, due to the fact that the contact stiffness was overestimated.

6. Conclusion

A two-stage interaction control scheme for a flexible arm whose tip is in contact with a compliant surface has been proposed in this paper. The first stage is in charge of solving the inverse kinematics problem to compute the desired vectors of the joint and the deflection variables that place the flexible arm tip at the desired position with the desired contact force. The solution is based on the transpose of a suitably modified arm Jacobian so as to account for the static effects due to gravity and contact force. The computed variables are used as the set-points for the second stage, which is a simple PD joint regulator. The attractive feature of the scheme is that it does not require force and deflection measurements. The price to pay is that an exact knowledge of the arm kinematic model, link stiffness and mass distribution as well as environment stiffness and position is required to guarantee accurate regulation of tip position and contact force.

Acknowledgements

This research is supported by *ASI* (Italian Space Agency).

References

Book, W. J. (1993). Controlled motion in an elastic world. *ASME Journal of Dynamic Systems, Measurement, and Control*, *115*, 252–261.

Canudas de Wit, C., Siciliano, B., & Bastin, G. (Eds.) (1996). *Theory of robot control*, London, UK: Springer.

De Luca, A., & Panzieri, S. (1996). End-effector regulation of robots with elastic elements by an iterative scheme. *International Journal of Adaptive Control and Signal Processing*, *10*, 379–393.

De Luca, A., & Siciliano, B. (1991). Closed-form dynamic model of planar multilink lightweight robots. *IEEE Transactions on Systems, Man, and Cybernetics*, *21*, 826–839.

De Luca, A., & Siciliano, B. (1993a). Regulation of flexible arms under gravity. *IEEE Transactions on Robotics and Automation*, *9*, 463–467.

De Luca, A., & Siciliano, B. (1993b). Inversion-based nonlinear control of robot arms with flexible links. *AIAA Journal of Guidance, Control, and Dynamics*, *16*, 1169–1176.

Khorrami, F., & Jain, S. (1993). Nonlinear control with end-point acceleration feedback for a two-link flexible manipulator: Experimental results. *Journal of Robotic Systems*, *10*, 505–530.

Siciliano, B. (1990). A closed-loop inverse kinematic scheme for on-line joint based robot control. *Robotica*, *8*, 231–243.

Siciliano, B. (1994). An inverse kinematics scheme for flexible manipulators. *Proceedings of the second IEEE Mediterranean symposium on new directions in control and automation*, Chania, GR (pp. 543–548).

Siciliano, B. (1998). An inverse kinematics scheme for a flexible arm in contact with a compliant surface. *Proceedings of the 37th IEEE conference on decision and control*, Tampa, FL (pp. 3617–3622).

Siciliano, B. (1999). Closed-loop inverse kinematics algorithm for constrained flexible manipulators under gravity. *Journal of Robotic Systems*, *16*, 353–362.

Siciliano, B., & Book, W. J. (1988). A singular perturbation approach to control of lightweight flexible manipulators. *International Journal of Robotics Research*, *7*(4), 79–90.

Vandegrift, M. W., Lewis, F. L., & Zhu, S. Q. (1994). Flexible-link robot arm control by a feedback linearization/singular perturbation approach. *Journal of Robotic Systems*, *11*, 591–603.